ChemComm

Accepted Manuscript

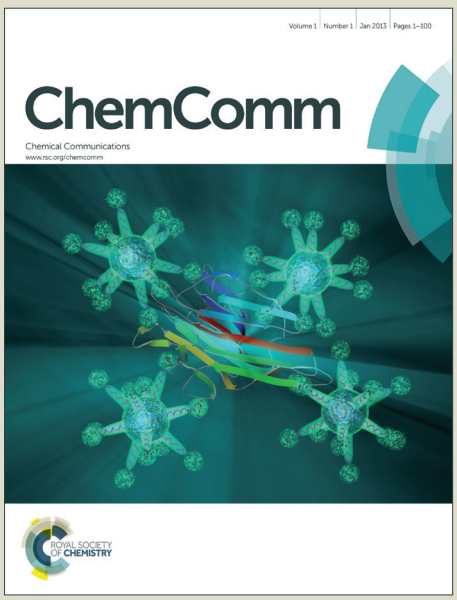

ROYAL SOCIETY OF CHEMISTRY

www.rsc.org/chemcomm

Journal Name

RSCPublishing

COMMUNICATION

Ultrasensitive room temperature NH_3 sensor based on graphene-polyaniline hybrid loading on PET thin film

zCite this: DOI: 10.1039/x0xx00000x

Shouli Bai[a], Yangbo Zhao[a], Jianhua Sun[a,b], Ye Tian[a], Ruixian Luo[a], Dianqing Li*[a], Aifan Chen*[a]

Received ooth January 2012,
Accepted ooth January 2012

DOI: 10.1039/x0xx00000x

www.rsc.org/

The motivation of this research is to develop a smart NH_3 sensor based on rGO-PANI hybrid loading on flexible PET thin film by in situ chemical oxidative polymerization. The sensor not only exhibits high sensitivity, good selectivity and fast response at room temperature but also has flexibility, cheap and wearable characteristics.

Ammonia (NH_3) as a common ingredient is widely used in various industries, but it irritates skin, eyes and respiratory tract of humans, if above its threshold of 25 ppm in air is quite dangerous for the human health.[1] At the present, most of the NH_3 sensors based on metal oxides, such as WO_3, ZnO, In_2O_3, etc. usually exhibit low sensitivity and high operating temperatures (200-450°C),[2] which results in high power consumption, safety hazard and low life time.[3] Hence, the development of a NH_3 sensor with high sensitive and operable at room temperature is very important, and need to aid of the conducting polymers. The main polymers that can act as gas sensing materials are polyaniline (PANI),[4] polypyrrole (PPy),[5] polythiophene (PTh) [6] and their derivatives.[7] Among them, PANI is considered to be the most promising and widely applied sensing material because of their low production costs, environmental stability and acceptable conductance, and it has unique sensing function to NH_3 gas. However, their low sensitivity and unsatisfying thermal stability restrict their application in practical sensors. Thus, many attempts have been made to improve the sensing performance of PANI, such as loading noble metals, added dopants or combining other components to construct composites, etc. Nevertheless, these efforts still face difficulties in getting a high response.

Graphene has emerged as a rapidly rising star in the field of material science because of its intriguing properties of high conductance, mechanical strength, and large specific surface,[8] but pristine graphene is seldom used directly as a starting material due to its poor dispersibility in most solvents. Delightfully, the graphite can be oxidized to be oxide graphite (GO) by modified Hummer's method.[9] Compared with pristine graphene, the oxygen functional groups in GO mostly in the form of hydroxyl and epoxy groups, render it strongly hydrophilic; this gives GO good dispersibility in many solvents, particularly in water, which provides reactive sites for the nucleation and growth of polymer, leading to the rapid growth of various grapheme-based hybrids.[10] However, on the other hand, the presence of these oxygenated functional groups in GO can indeed give rise to remarkable structure defects, this is concomitant with some loss in electrical conductivity, which possibly limits the direct application of GO in electrically active materials and devices.[11] Recently, it has been demonstrated that reduction of GO transforms the sp^3 hybridized carbon to sp^2, leading to the restoration of conjugation and hence a high electrical conductivity can be realized.[12] Thus, chemical reduction was employed to synthesize rGO. Meanwhile, the reduced graphene oxide (rGO) can be functionalized by blending with other sensing components to modulate its structure and improve the sensing performance of the hybrid. Therefore, combining the characters of the PANI and rGO will generates novel sensing materials, which over the constituent counterparts in the work.

More importantly, the concept of this work is to use a flexible and cheap polyethylene terephthalate (PET) thin film as sensor substrate. Compared with indium-tin oxide (ITO), fluorine doped tin oxide (FTO), glass and paper substrates, the PET have the advantages of high transparency, good flexibility, and low cost. PET substrate of large area is commercially available, which is a good substrate for fabrication of flexible and wearable sensors.

A series of rGO-PANI hybrids have been synthesized by a facile chemical oxidative polymerization. The route synthesized rGO-PANI hybrid is shown in Scheme 1. The thin film sensors of pure PANI and rGO-PANI hybrids loading on PET substrate have been fabricated and attached on the probes of the devices with silver paint (the experimental detail, see the ESI).

In the process of preparing rGO-PANI hybrid, rGO aqueous solution was added into acidic solution containing aniline monomers. Aniline in HCl solutions gets one proton to be an anilinium cation ($C_6H_5NH_3^+$). Owing to the incomplete chemical reduction, a small portion of residual

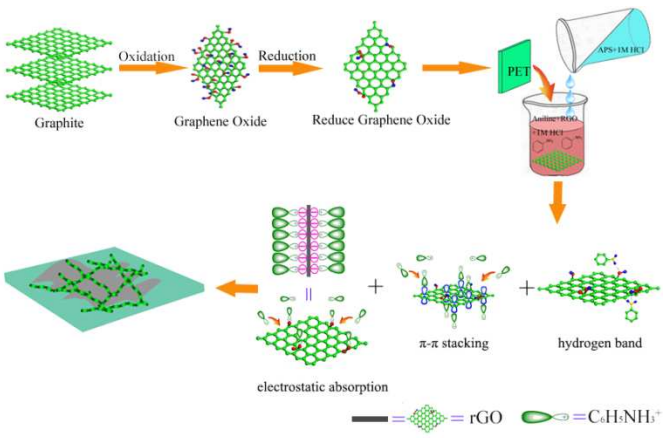

Scheme 1. Schematic diagram of the preparation process for rGO-PANI hybrid.

oxygen functional groups still exist in rGO[13]. These residual oxygen functional groups in rGO combined with anilinium cations to produce the rGO-PANI hybrid through electrostatic interaction (doping process), hydrogen bonding, and π-π stacking interaction between them.[14] As a result, the anilinium cation grows on the surface of rGO. Subsequent the addition of ammonium peroxydisulphate (APS) makes the aniline monomers polymerized.

The structure of as-prepared materials was investigated by powder X-ray diffraction (XRD) analysis. The XRD patterns of PANI and 1.0 wt % rGO-PANI (PRG1.0) hybrid are shown in Fig. 1a. The XRD pattern of PANI showed three characteristic peaks. The characteristic peaks at 2θ=15.2° and 25.4° are attributed to the periodicity both perpendicular and parallel to the polymer chain, respectively.[15] The peak at 2θ of 20.4° is caused by the layers of polymer chains at alternating distances.[16] The XRD pattern of PRG1.0 has similar peaks as PANI, excluding the slight shift about the position of peak due to the incorporated effect of rGO in the hybrids. Fig.1b demonstrates the Raman spectra of rGO, PANI, and PRG1.0. The Raman spectrum of as-prepared rGO displays two prominent peaks at 1346 and 1594 cm^{-1} that

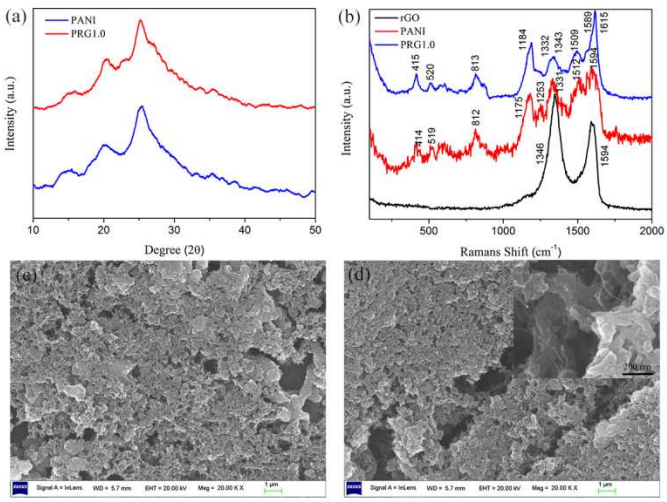

Fig.1 (a) XRD patterns of PANI and PRG1.0; (b) Raman spectra of rGO, PANI, and PRG1.0; (c) SEM image of PANI; and (d) SEM image of PRG1.0.

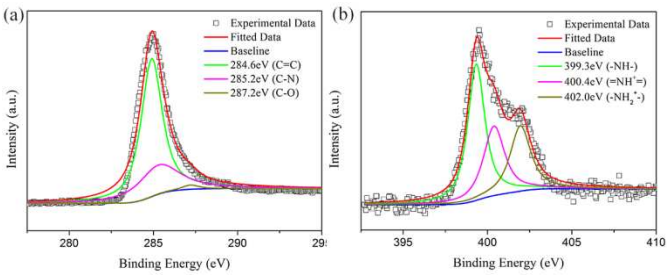

Fig.2 XPS spectra of (a) the C1s region of RPG1.0 and (b) N1s region of PRG1.0.

correspond to the D and G modes, respectively.[17] For pure PANI, out-of-plane C−H wag, out-of-plane C−N−C torsion, imine deformation, in-plane C−H bending, in-plane ring deformation, C−$N^{+\cdot}$ stretching, C═N stretching of quinoid, C−C stretching of benzoid situated at 416, 517, 813, 1175, 1253, 1331, 1512, and 1594 cm^{-1} are observed.[14] The peaks shift to 415, 520, 813, 1184, 1332, 1509 and 1589 cm^{-1} when rGO was introduced into the synthesis process of rGO-PANI hybrid. This is probably due to the doping of carboxyl acid of rGO to PANI backbone and π−π stacking of PANI and rGO sheets.

Several analytical techniques were further employed in sample characterization. The morphology and structure of the PANI and PRG1.0 hybrid were characterized using scanning electron microscope (SEM). The results are shown in Fig.1c-d. The pure PANI shows uniform fibrous structures of 200 nm in length and about 50 nm in width. For PRG1.0 hybrid, SEM image shows that all the rGO sheets are homogeneously surrounded with PANI. This morphology of PANI remains same in the PRG1.0 hybrid, indicating that the synthesis process do not have a significant effect on the morphology of the PANI.

Surface sensitive X-ray photoelectron spectroscopy (XPS) is used to reveal the different electronic structures and chemical bond information of as-prepared materials. To further determinate the chemical bond state of carbon in rGO-PANI hybrid, the comparison of the C1s core level of GO (Fig. S1) and PRG1.0 (Fig. 2a) was made. The C1s of XPS spectrum of GO (Fig. S1) can be deconvoluted into five Gaussian peaks at 284.5, 285.3, 286.3, 287.1 and 288.3 eV, which attributed to the typical signals of C-C, C–OH, C-O, C=O and O-C=O, respectively.[18] Meanwhile, the detected carbon element in the PRG1.0 is revealed from the C=C band at 284.5 eV and C–N band at 285.2 eV of the core-level C1s XPS spectrum.[19] However, it is noteworthy that there remains a weak C–O band at 287.2 eV, which may be assigned to the residual hydroxyl or epoxy groups on the rGO sheets. Such residual groups may form hydrogen bonds with the polyaniline, and then bring another intimate interaction between rGO and PANI besides the π–π electron stacking.[14] In addition, the significant decrease signal of the oxygen-containing groups in the PRG1.0 demonstrates a high degree of deoxygenating and successful reduction from GO to rGO during the chemical reduction process, which effectively increases the electrical conductivity of rGO-PANI hybrids. The N1s core level of PRG1.0 (Fig. 2b) is detected. The asymmetric N1s core level of PRG1.0 is composed of three peaks centred at about 399.3 eV (-NH-), 400.4 eV (=NH^{+}=) and 402.0 eV (-NH_2^{+}-),[20] respectively. The area fraction of these three peaks is 0.367, 0.352 and 0.281, respectively, where the total area from protonated nitrogen atoms is 63.3%, indicating that the doping level of polyaniline in PRG1.0 hybrid is 63.3%.[21]

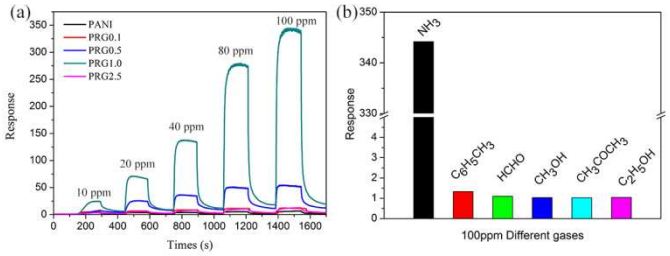

Fig. 3 (a) The transient sensing characteristics of PANI-PET thin film and hybrids-PET thin films to 10-100 ppm NH_3; (b) The selectivity of PRG1.0 to 100 ppm different gases.

The sensing responses of the sensors based on PANI-PET and hybrids-PET films were measured by exposing in different concentrations of NH_3 gas at room temperature (22.0 °C), as shown in Fig.3a. Amazingly, the resistance immediately increases when the sensor was exposed in NH_3 and rapidly recovers with the withdrawal of NH_3. For a reducing gas of NH_3, the sensor response is defined as "Response=R_{gas}/R_{air}" where R_{gas} is the resistance in the presence of the NH_3 gas and R_{air} is the resistance in air. According to above equation, the response of PANI-PET thin film is 6.7 to 100 ppm of NH_3, while the highest response is up to 344.2 for PRG1.0-PET thin film, which is 51 times higher than that of the PANI-PET thin film. From fig. 3(a), the response of PRG1.0-PET thin film to NH_3 is the highest among all the studied samples, so the optimum amount of rGO in hybrids is 1.0 wt%.

The response and recovery times are also important parameters for a gas sensor, which were defined as the time to reach 90% of the final equilibrium value after the detected gas was injected and removed, respectively. The response and recovery times of PANI-PET thin film to 100 ppm of NH_3 are 52 s and 80 s, respectively, while the response and recovery times of PRG1.0-PET thin film are 20 s and 27 s, respectively (Fig. S2, ESI). In addition, the response time and recovery time of PRG1.0-PET thin film along with various concentrations of NH_3 are summarized (Fig. S3, ESI). With the increase in NH_3 concentration, the response time and recovery time decrease. For comparison, the sensing properties to NH_3 for several hybrids of PANI with metal oxides or with rGO have been summarized (Table 1, ESI).[22] From Table 1, it is apparent that the PRG1.0-PET thin film shows good NH_3-sensing performances than previously reported hybrids. Besides, the response time is among the faster values, and the recovery times in our work are shorter than most of the reported. It is well known that high selectivity is an important factor for a practical and valuable gas sensor. Therefore, the selectivity data of the PRG1.0-PET thin film to ethylbenzene, methanol, formaldehyde, ethanol and acetone (VOCs) at room temperature are shown in Fig. 3b, they are 258, 312, 333, 336 and 330, respectively to 100 ppm NH_3. Such high selectivity results from the difference of their sensing mechanism.The acid–base deprotonation process of PANI nanoparticles plays an important role in the enhancement of the sensing performance after exposure of the sensor to NH_3, resulting in the selective response to NH_3 gas (Fig.S4, ESI).[23] While the sensing mechanism of hybrid to VOCs results from the gas surface adsorption and oxidizing reaction of gas with adsorbed oxygen species. This is why the rGO-PANI hybrids have excellent selectivity.

The improvement of gas-sensing properties may be attributed to four reasons: 1) A large specific surface area of the hybrid can be achieved due to the PANI nanoparticles are anchored on the surface of rGO sheets, which is of benefit to the adsorption of NH_3 gas on hybrid surface and the deprotonation at the interface of hybrid. Since the sensing process of such sensor involves adsorption/desorption phenomena and deprotonation at the interface, the large specific surface area of gas sensing materials is crucial to maintain their high sensing performance.[24] 2) The rGO sheets provide high carriers mobility at room temperature, which results in the rapid increase of the hybrid resistance, that is, reduces the response time of hybrid toward NH_3 gas;[25] 3) When rGO sheets expose to NH_3 gas, it will cause decrease in the number of charge carriers due to the electron withdrawing nature of absorbed water, which induce hole-like carriers,[26] resulting in an increase in resistance, thus increasing the sensitivity to NH_3 gas[26]; 4) The electron transfer may occur between the conjugated PANI and rGO through π-π interaction during the sensing process, and consequently increases the sensing performance of hybrid.[27] However, detailed understanding for the role of rGO in the sensing mechanism of hybrid is still lacking. Moreover, herein report smart sensor has many advantages such as low cost, easy fabrication, flexibility, and mainly in wearable technology. These can be in the form of smart shirts which allows the continuous monitoring of hazardous gases like NH_3.

In summary, a series of rGO-PANI hybrids were synthesized by a facile, *in situ* chemical oxidative polymerization. The NH_3 sensors based on rGO-PANI hybrids loading on flexible PET thin film have been fabricated successfully. Among them, the PRG1.0 hybrid based sensor exhibits the highest response of 344.2 to 100 ppm NH_3, excellent selectivity to some of VOCs and rapid response, the response time and recovery time is 20 s and 27 s, respectively at room temperature. The enhancement of sensing properties for the resulting hybrid can be attributed to the synergetic effects between the rGO and the PANI. So, the PRG1.0 hybrid is a promising sensing material for detection of low concentration NH_3.

This work was supported by the National Natural Science Foundation of China (Grant Nos. 21177007 and 51372013), the Fundamental Research Funds for the Central Universities (YS1406), Guangxi Key Laboratory of Petrochemical Resource Processing and Process Intensification Technology, Guangxi University and Beijing Key Laboratory of Environmentally Harmful Chemicals Analysis.

Notes and references

[a] *State Key Laboratory of Chemical Resource Engineering, Beijing University of Chemical Technology, Beijing 100029, China. Fax/Tel: 86 010 64436992; E-mail: luorx@mail.buct.edu.cn; lidq@mail.buct.edu.cn.*
[b] *Guangxi Key Laboratory of Petrochemical Resource Processing and Process Intensification Technology, School of Chemistry and Chemical Engineering, Guangxi University, Nanning 530004, China*

†Electronic Supplementary Information (ESI) available: Experimental details and supporting figures. See DOI: 10.1039/b000000x/

1 B. Timmer, W. Olthuis and A. v. d. Berg, *Sens. Actuators. B*, 2005, **107**, 666.
2 (a) M. D'Arienzo, L. Armelao, C. M. Mari, S. Polizzi, R. Ruffo, R. Scotti and F. Morazzoni, *J. Am. Chem. Soc.*, 2011, **133**, 5296; (b) L. Wang, Z. Lou, T. Fei and T. Zhang, *J. Mater. Chem.*, 2012, **22**, 4767; (c) S. Elouali, L. G. Bloor, R. Binions, I. P. Parkin, C. J. Carmalt and J. A. Darr, *Langmuir*, 2012, **28**, 1879.

3 (a) Y. C. Her, B. Y. Yeh and S. L. Huang, *ACS Appl. Mater.Interfaces*, 2014, **6**, 9150; (b) F. Mendoza, D. M. Hernández, V. Makarov, E. Febus, B. R. Weiner and G. Morell, *Sens. Actuators. B*, 2014, **190**, 227.
4 J. Qi, X. Xu, X. Liu and K. T. Lau, *Sens. Actuators. B*, 2014, **202**, 732.
5 S. T. Navale, A. T. Mane, M. A. Chougule, R. D. Sakhare, S. R. Nalage and V. B. Patil, *Synthetic Met.*, 2014, **189**, 94.
6 S. T. Navale, A. T. Mane, G. D. Khuspe, M. A. Chougule and V. B. Patil, *Synthetic Met.*, 2014, **195**, 228.
7 (a) S. Nasirian and H. Milani Moghaddam, *Polymer*, 2014, **55**, 1866; (b) S. T. Navale, G. D. Khuspe, M. A. Chougule and V. B. Patil, *RSC Advances*, 2014, **4**, 27998; (c) S. Bai, K. Zhang, J. Sun, D. Zhang, R. Luo, D. Li and C. Liu, *Sens. Actuators. B*, 2014, **197**, 142.
8 M. Pumera, *Chem. Soc. Rev.*, 2010, **39**, 4146.
9 Y. Zhang, K. Fugane, T. Mori, L. Niu and J. Ye, *J. Mater. Chem.*, 2012, **22**, 6575.
10 Q. Xiang, J. Yu and M. Jaroniec, *Chem. Soc. Rev.*, 2012, **41**, 782.
11 D. Chen, H. Feng and J. Li, *Chem. Rev.*, 2012, **112**, 6027.
12 R. S. Dey, S. Hajra, R. K. Sahu, C. R. Raj and M. K. Panigrahi, *Chem. Commun.*, 2012, **48**, 1787.
13 K. Zhang, L. L. Zhang, X. S. Zhao and J. Wu, *Chem. Mater.*, 2010, **22**, 1392.
14 H. Wang, Q. Hao, X. Yang, L. Lu and X. Wang, *ACS Appl. Mater. Interfaces*, 2010, **2**, 821.
15 Y. Li, X. Zhao, P. Yu and Q. Zhang, *Langmuir,* 2013, **29**, 493.
16 Y. Li, X. Zhao, Q. Xu, Q. Zhang and D. Chen, *Langmuir*, 2011, **27**, 6458.
17 W. Yuan, A. Liu, L. Huang, C. Li and G. Shi, *Adv. Mater.*, 2013, **25**, 766.
18 K. Chi, Z. Zhang, J. Xi, Y. Huang, F. Xiao, S. Wang and Y. Liu, *ACS Appl. Mater. Interfaces.*, 2014, **6**, 16312.
19 S. Golczak, A. Kanciurzewska, M. Fahlman, K. Langer and J. Langer, *Solid State Ionics*, 2008, **179**, 2234.
20 D. Xu, Q. Xu, K. Wang, J. Chen and Z. Chen, *ACS Appl. Mater. Interfaces*, 2014, **6**, 200.
21 Z. Tong, Y. Yang, J. Wang, J. Zhao, B.-L. Su and Y. Li, *J. Mater. Chem. A*, 2014, **2**, 4642.
22 (a) Z. Wu, X. Chen, S. Zhu, Z. Zhou, Y. Yao, W. Quan and B. Liu, *Sens. Actuators. B*, 2013, **178**, 485; (b) J. Luo, Y. Chen, Q. Ma, R. Liu and X. Liu, *J. Mater. Chem. C*, 2014, **2**, 4818.
23 S. Virji, J. Huang, R. B. Kaner and B. H. Weiller, *Nano Lett.*, 2004, **4**, 491.
24 S. Deng, V. Tjoa, H. M. Fan, H. R. Tan, D. C. Sayle, M. Olivo, S. Mhaisalkar, J. Wei and C. H. Sow, *J. Am. Chem. Soc.*, 2012, **134**, 4905.
25 X. Huang, X. Qi, F. Boey and H. Zhang, *Chem. Soc. Rev.*, 2012, **41**, 666.
26 R. K. Joshi, H. Gomez, F. Alvi and A. Kumar, *J. Phys. Chem. C*, 2010, **114**, 6610.
27 X. Huang, N. Hu, R. Gao, Y. Yu, Y. Wang, Z. Yang, E. Siu-Wai Kong, H. Wei and Y. Zhang, *J. Mater. Chem.*, 2012, **22**, 22488.

